

Optical and Structural Study of the CZTS ($\text{Cu}_2\text{ZnSnS}_4$) Thin Film for Solar Cell Derived from the Chloride-Based sol-gel Precursor Solution

M Rahman¹, M S Bashar², and N Islam^{1*}

¹ Department of Physics, Dhaka University, Dhaka-1000, Bangladesh

² IFRD, BCSIR, Dhaka, Bangladesh

(Received: 18 March 2021; Accepted: 6 April 2022)

Abstract

Fabrication of environmentally safe $\text{Cu}_2\text{ZnSnS}_4$ (CZTS) photovoltaic thin films of pure kesterite state is crucial. We have prepared CZTS thin films by sol-gel dip-coating process from chloride-based chemicals. After vacuum-annealed at 550°C, the optical and structural characters of the films were further examined by UV-vis spectroscopy, X-ray diffraction (XRD), scanning electron microscopy (SEM), and energy dispersive X-ray spectroscopy (EDS) methods. The CZTS films offered high optical absorption ($0.4 \times 10^4 \text{ cm}^{-1}$) and nearly optimum bandgap energy (1.65 eV). X-ray diffraction examination confirmed the kesterite structure of films. Scanning electron micrograph affirmed the creation of jam-packed, condensed and granulated CZTS films. The thin film displayed intermittent disposal of agglomerated particles with clear-cut edges. The energy dispersive X-ray spectroscopy study gave the stoichiometric ratio as Cu: Zn: Sn: S = 2.2: 1.4: 1: 5.1.

Keywords: Thin film, Sol-gel, Absorption layer, Solar cell, $\text{Cu}_2\text{ZnSnS}_4$, XRD, SEM, EDS.

I. Introduction

Over the last decade, research, evolution and industrialization of thin film photovoltaic technology have been flourishing because of manufacturing cost-reduction, utilization of environmentally-safe materials and scalable design. We should mainly consider the cost reduction and scalability factors for making photovoltaic technology to challenge the fossil fuels¹. The modern polycrystalline thin film photovoltaic cells – gallium arsenide (GaAs), cadmium telluride (CdTe), copper indium selenide (CIS) and copper indium gallium selenide (CIGS) - have evolved financially feasible units. Despite having medium power conversion efficiencies (PCE) - >11% in unit manufacturing and 20% in workshop – CdTe and CIGS are un-livable to ultimate terawatt-scale manufacturing because of scarcity and cost of Te, In, and Ga¹⁻⁵. Moreover, Cd, Se and As are highly toxic elements that produce health hazards for animals and human beings. Hence, fabrication of thin film solar cells from the earth abundant as well as non-toxic elements is a crucial challenge. CZTS ($\text{Cu}_2\text{ZnSnS}_4$) is popping up as the ‘next generation’ solar absorber which has similar structure to CIGS, but contains non-toxic and earth rich (Cu: 50 ppm, Zn: 75 ppm, Sn: 2.2 ppm, S: 260 ppm)⁶ elements. CZTS has other advantages too – best direct band gap energy (1.4 ~ 1.6 eV), great absorption coefficient ($>10^4 \text{ cm}^{-1}$) and hypothetical high energy transformation efficiency (~ 32.2%)^{3, 7-9}.

Researchers have adopted several deposition techniques – pulsed laser deposition¹⁰, thermal evaporation¹¹, chemical vapour deposition¹² and sputtering deposition¹³ – for construction of CZTS thin films. Nonetheless, thin film deposition facility yet necessitates rigorous processing conditions to get acceptable efficacy which eventually increase fabrication cost. Therefore, many researchers have

prepared CZTS films in non-vacuum conditions¹⁴⁻¹⁶ to reduce the cost. To date, CZTS thin-film solar cells produced under a hydrazine-based non-vacuum condition gave best results (PCE – 12.6%^{17,18}). But, the PCE of CZTS is yet lower than that of CIGS ($\eta > 21\%$)^{19,5}. Moreover, hydrazine is extremely harmful and fickle compound which necessitate high storage care²⁰. Hence, we need a robust, easily scalable, and environmentally safe solution-based technique for manufacturing of the CZTS thin films to get high efficiency.

Other factors also affect the performance of CZTS thin-film photovoltaic cells: low open circuit voltage (VOC)²¹, low minority carrier lifetime of about several nanoseconds²² and adversity in the evolution of a true CZTS state from Cu, Zn, Sn, and S.

The elements of CZTS thin films forms many secondary phases during the fabrication²³ – a Cu-abundant composition creates a Cu_2S auxiliary state while Sn- and Zn-abundant design create SnS and ZnS secondary phases, respectively^{24, 25} which negatively impact the performance of the cells.

Appropriate configuration of CZTS thin-film photovoltaic cells is yet unspecified. The CZTS thin film is a kesterite-structured complex material and exposed to deformity. Moreover, change of precursor conditions affect the phase creation of kesterites which eventually influence the efficacy of photovoltaic cells. As a whole, scientists have reported Cu-abundant and Zn-abundant compositions of CZTS photovoltaic cells give high efficiency^{3, 18, 22, 26-29}. But, Hsu et al. reported Cu-abundant and Zn-abundant photovoltaic cells having a near perfect stoichiometric configuration give low efficacy³⁰.

In this research, we have reported the sol-gel dip-coating technique to fabricate CZTS thin films absorption layer

*Author for correspondence. e-mail: naimulphy@du.ac.bd

applying 2-methoxyethanol being solvent and mono-ethanolamine (MEA) being the stabilizer. MEA have a function in the growth of durable CZTS sol-gel precursor and manufacturing good character CZTS films. Later, we explored the structural and optical features of the thin films.

II. Experimental Procedures

First, the substrate was wiped carefully with a tissue paper soaked with methanol and deionized water respectively. After that, the glass slide was submerged in methanol for few minutes and followed by an ultrasonic bath for 10 minutes. Similarly, the glass slide was submerged in acetone and DI water respectively for few minutes followed by an ultrasonic bath for 10 minutes in both cases.

The precursor solution was made of Copper (II) Chloride Dihydrate (1.8M), Zinc Chloride (1.2M), Tin (II) Chloride Dihydrate (1M), Thiourea (8M), 2-methoxyethanol, and Monoethanolamine³¹. Thiourea was used as the source of sulfur. The solutes were dissolved in 2-methoxyethanol. The 2-methoxyethanol acted as a solvent and few drops of mono-ethanolamine being a mediator for the precursor solution. The solution was stirred by a magnetic stirrer for homogenous and continuous mixing of the chemicals. The solutions were stirred until the solution temperature reached to 70°C. Then, the solutions were further stirred for another 30 minutes at a constant temperature of 70°C.

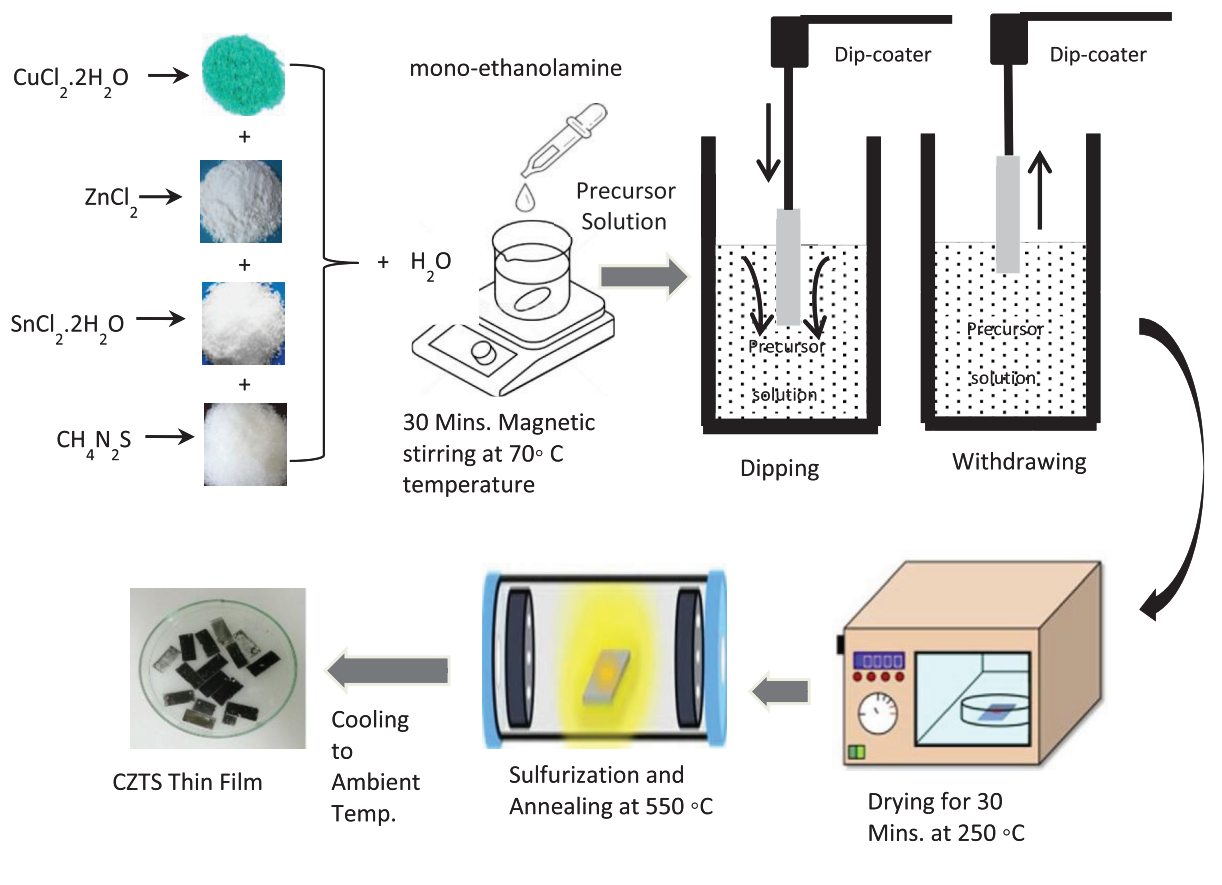


Fig. 1. Synthesis process of CZTS thin films is laid-out in the diagram: preparation of precursor solution, deposition of CZTS films on glass substrate through dip coating method, drying and annealing. The deposited CZTS thin films are finally presented in a petri dish in the diagram.

The CZTS thin films were produced from the chloride-based sol-gel precursor solution on glass substrates. Each glass substrate was dipped for 3 minutes into the sol-gel precursor Fig. 1. The glass slides were dipped into and picked up at three different dipping speeds. Depending on this speed the samples were labelled as sample 1, 2 and 3 respectively. The deposited glass slides were put into an oven for drying after raising the starting temperature of the oven to 150°C. Then the temperature was raised to 250 °C and all the slides were

put in the oven for 30 minutes to clear away the solvent and constituent elements from the CZTS thin films. The dried CZTS thin films were sulfurized in an annealing chamber at 550 °C, and then cooled down to the ambient condition.

The thickness “*d*” of the films was measured by using a stylus profiler (BRUKER Dektak XT™, Germany). The optical characteristics i.e. transmittance, reflectance, and absorbance were measured using the UH4150, Hitachi, UV-

vis spectrophotometer (Japan). The measured wavelength range was from 300 to 700 nm. The X-ray diffraction method was applied to study the structural characteristics of the CZTS films. The diffraction pattern was recorded using the GBC (Australia) system. The Cu-K α emission was employed to get the possible fundamental diffraction peaks from the sample. The SEM EVO 18, Zeiss (Germany) high-performance scanning electron microscope was employed to study the surface morphology and uniformity of the deposited CZTS thin films.

III. Results and Discussion

Thickness

Thickness is a critical criterion for the CZTS thin films. Characteristics of CZTS thin film differ in thickness since surface conditions change. To observe the change of film-thickness of the CZTS films with dip-coating speed, we prepared multiple samples from the same chemical with

different dip-coating speeds. The film thickness did not vary significantly with dipping speeds. We obtained the average thickness of the CZTS film as 10.34 μm . Usual absorption coefficients for the CZTS thin films has a range: 10^4 - 10^5 cm^{-1} and a bulky absorber adequately take in the solar spectrum and cut down recombination – increase the minority carrier lifetimes – at the back contact^{34, 35}. Todorov et al. suggested that absorber thickness greater than 2.5 μm would increase the efficiency of the CZTS thin film³⁶. We have shown the picture of homogeneous and solid CZTS thin films at 50, 75 and 100 ms^{-1} dipping speed onto the clean glass substrate in Fig. 1. The big glass substrate area –10 cm^2 – indicates the practicability of sol-gel technique for big size CZTS film development.

Optical Studies

The variation of the optical absorbance, transmittance, and reflectance with wavelengths of CZTS thin films prepared from the chloride based precursors are shown in Fig. 2.

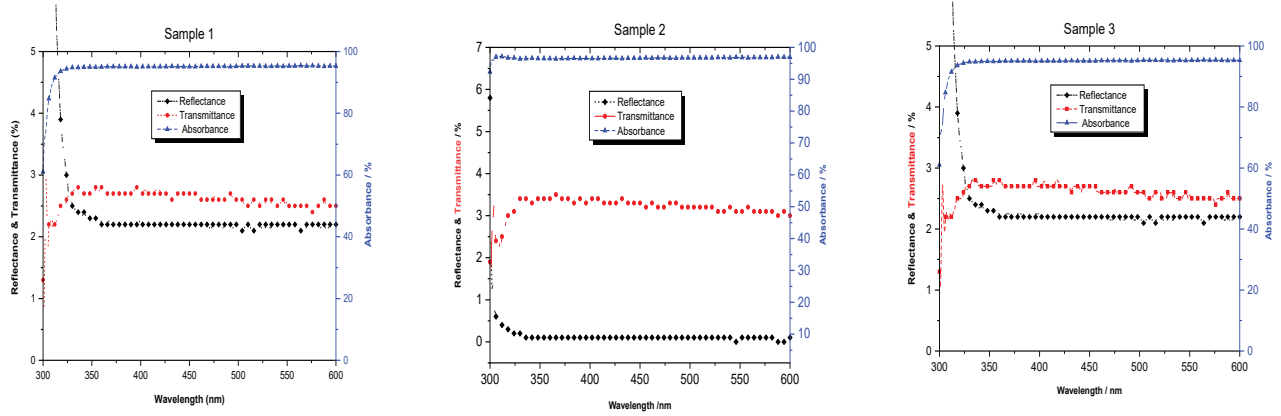


Fig. 2. Absorbance, transmittance and reflectance variation of the CZTS films with the wavelengths of three samples 1, 2 & 3 prepared at dip coating speed 100, 75 & 50 ms^{-1} respectively.

The spectra disclosed very high absorbance (95.75, 98.3 and 95.9%) and both very low transmittance (2.75- 3.8%, 0.75 -1.15% and 3.1-3.4%) and reflectance (0.65-0.85%, 0.4 -0.5%, and 0.6-0.81%) respectively for sample 1, 2 and 3 of the CZTS thin films of at visible EM wave range. These indicated the relevance as an absorber layer for photovoltaic cells of these types of thin films.

We computed the absorption coefficients “ α ” of the CZTS thin films from the experimental absorbance data, obtained at specific wavelengths linked to specific photon energies at room temperature. We have exploited the Beer-Lambert law³:

$$a = 2.303 \frac{A}{d} \quad (1)$$

Where, ‘ A ’ = $\log_{10} \left(\frac{I_0}{I} \right)$ represents absorbance, ‘ d ’ represent film-thickness, ‘ I ’ represents the light intensity passing through the CZTS film and ‘ I_0 ’ represents incident light intensity.

The average “ α ” of the CZTS thin films was $0.4 \times 10^4 \text{ cm}^{-1}$. All these “ α ” values were close to the standard value – 10^4 cm^{-1} for the CZTS thin films³⁷. The obtained “ α ” values less than 10^4 cm^{-1} for the chloride based CZTS thin films is consistent with other published research works¹. Therefore, our work confirmed that the produced thin film is suitable for solar energy transformation.

We determined the band gap energy “ E_g ” using the absorption coefficient values¹. The absorption coefficient “ α ” is linked to the photon energy “ $h\nu$ ” by the equation below:

$$a = \frac{A_0 (h\nu - E_g)^n}{h\nu} \quad (2)$$

Where ‘ A_0 ’ is a constant linked to the effective masses which is associated with bands, n . Depending on bandgap materials⁷- direct or indirect- ‘ n ’ can have value either 0.5 or 2. So we have assumed ‘ n ’ = 0.5 for CZTS being a direct bandgap material. Simplifying equation 2, we get

$$a = \frac{A_0(h\nu - E_g)^{0.5}}{h\nu} \quad (3)$$

$$(\alpha h\nu)^2 = A_0^2 (h\nu - E_g) \quad (4)$$

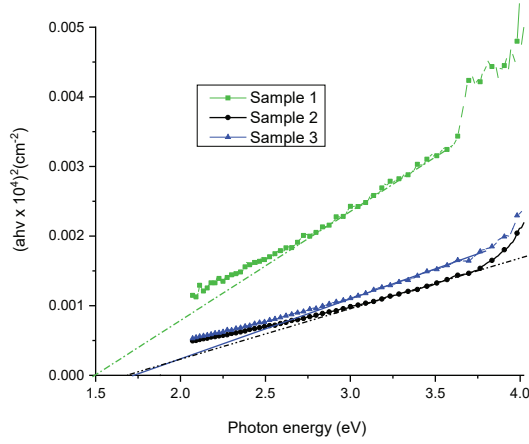


Fig. 3. Tauc plot of the CZTS thin films prepared from the chloride chemical-based precursor solution

We estimated the optical bandgap energy using equation 4. The $(\alpha h\nu)^2$ values were plotted against photon energy ($h\nu$), which is known as the Tauc plot. The bandgap energy value is obtained through extrapolation of the linear part of the Tauc plot to until it intercepts the photon energy axis. Fig.3 presents the changes of $(\alpha h\nu)^2$ value against $h\nu$, which shows a linear rise in the higher energy territories - indicate a straight optical transition. Through projections, we got the average bandgap energies and average value obtained, was 1.65 eV. Our bandgap value concurred with bandgaps notified for CZTS films by many separate authors^{2, 3, 7, 25, 37-43, 49-51}. Our obtained bandgap is near to the ideal band gap (1.5 eV)⁴⁴ required for a solar cell which indicate the suitability of CZTS material for thin film solar cell application.

Structural Studies

Sulfurization of the CZTS films at 550°C for 30 minutes improved crystallinity of the films. Without sulfurization, the deposited CZTS film showed no diffraction peaks. For structural studies only sample 2 (dip coating speed, 75ms⁻¹) was chosen since it gave the highest absorbance (98.3%) and optimum bang gap (close to 1.5eV). Fig. 4 presents the XRD patterns of sulfurized CZTS thin films. The CZTS films have the primary characteristics diffraction peaks at angles $2\theta = 28.4^\circ, 31.84^\circ, 32.898^\circ, 47.25^\circ$ and 56.10° along the (112), (103), (200), (220) and (312) planes, respectively. The XRD spectra reaffirmed the polycrystalline character with kesterite tetragonal crystal structure³⁸ [JCPDS card no. 26-0575] of the CZTS film. We calculated the lattice parameters from the XRD spectral information using the equation 5 for each CZTS sample:

$$\frac{1}{d^2} = \frac{h^2 + k^2}{a^2} + \frac{l^2}{c^2} \quad (5)$$

Where $h, k,$ and l are the Miller indices of the crystal planes. The “ a ” and “ c ” are lattice parameters, which are constant for the specific thin film and “ d ” is the observed spacing given by,

$$d = \frac{\lambda}{2 \sin \theta} \quad (6)$$

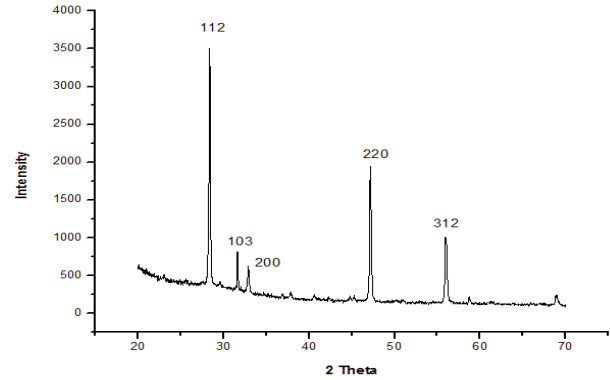


Fig. 4. The XRD patterns of the sulfurized CZTS thin films prepared from the chloride chemical based precursor

To get the value of d , the value of λ ($= 0.15406\text{nm}$) and θ (taken from the XRD graph) were put in equation 6. The values of d are put in equation 5 and six different equations were obtained. To determine the lattice parameters ‘ a ’ & ‘ c ’, the Miller indices $h, k,$ and l values ((112), (103), (220) and (312)) were used in these six equations. Finally, solving these six equations the values of ‘ a ’ & ‘ c ’ were obtained. The average value of “ a ” obtained – 0.5431 nm, which is very close to the ideal value of the lattice parameter – “ $a_0 = 0.5435\text{nm}$ ” – of the CZTS crystal^{6, 9}. The lattice parameter “ c ” of the CZTS kesterite crystal was also determined and the average value of “ c ” was 1.064235 nm. The obtained value of the lattice parameters “ c ” of the CZTS crystal was very close to the standard value of the lattice parameter “ $c_0 = 1.0843\text{nm}$ ”^{6, 9}.

We also determined the grain size from the ‘full width at half maxima (FWHM)’ of diffraction peaks. Debye and Scherrer first worked out it in the following manners:

$$D = \frac{0.94\lambda}{\beta \cos(\theta)} \quad (7)$$

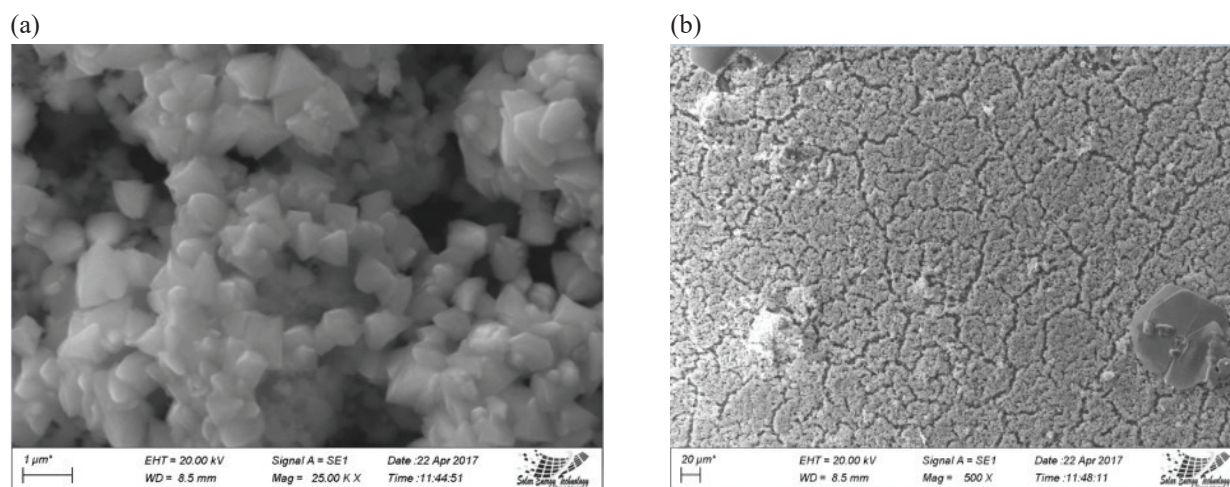
Where ‘ D ’ is the mean particle size and ‘ β ’ is the FWHM of the peak of (hkl) plane.

The obtained average grain dimension of the CZTS thin films was 34.21 nm.

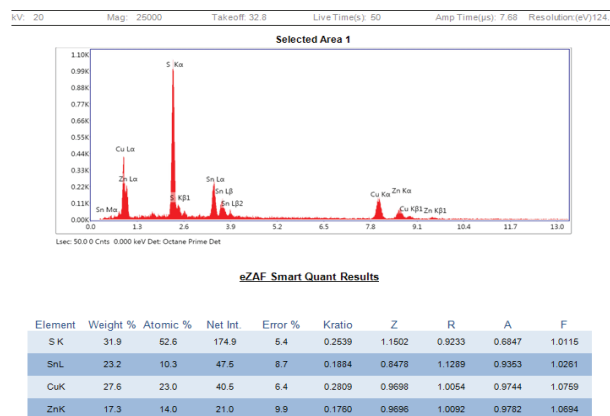
The calculated lattice parameters and grain size for each type of sample are tabulated in Table 1

Table 1. Lattice parameters of the deposited CZTS thin films

d /nm	hkl	$2\theta / ^\circ$	'a' /nm	Average 'a' /nm	'c' /nm	Average 'c' /nm	Standard 'a' /nm	Standard 'c' /nm	$\beta / ^\circ$	D /nm	Average D /nm
0.3162	112	28.2	0.542	0.5431	1.11965	1.0643	0.5435	1.0843	0.201	42.78	34.21
0.282	103	31.725	0.5438		0.98196				0.2308	39.72	
0.2715	200	32.92	0.542						0.533	17.84	
0.1923	220	46.24	0.5435						0.2404	37.67	
0.164	312	56.055	0.544		1.09115				0.2846	33.03	

Surface morphology and compositional studies**Fig. 5.** The surface morphology of the CZTS thin film [(a) 20000X (b) 500X].

We examined the superficial architecture and constituent analysis. For this, we took the sample 1 because of its highest absorbance and optimum bandgap. Fig. 5 (a & b) displays the scanning electron micrographs of the thin films at two distinct magnifications. The Scanning Electron Microscope pictures (Fig.5 (a & b)) endorsed the compact and dense nature of the films. The films have irregular disposal of agglomerated particles with clear cut borders. Big agglomeration of molecule was observed in the Scanning Electron Microscope images; and according to Zao et al⁴⁵, and Ford et al⁴⁶, large agglomeration reduces the recombination rate of photo generated electron hence strongly supports its benefit in photovoltaic applications. The Scanning Electron Microscope picture also disclosed that the CZTS thin films hold good uniformity and surface flatness (Fig.5 a& b). Our findings conformed to the findings of others. Caballero et al.⁴⁷ got an identical kind of homogeneous, polycrystalline and compact CZTS thin films. Riha et al.⁴⁸ formulated a jam-packed nanocrystals that has balanced distribution of particle everywhere on the surface and lacked any fracture or gaps. Pawar et al.⁴⁴ found analogous grains for CZTS films formulated by electro-deposition process being there complexing agent. Wangperawong et al.⁴⁹ presented alike densely filled design for $\text{Cu}_2\text{ZnSnS}_4$ taken away aqueous bath means.

**Fig. 6.** EDS image and content scrutiny of the CZTS thin films

We did the elemental scrutiny of the harden CZTS thin film by EDS technique. The obtained atomic weight percentage ratio of the CZTS thin film – Cu: Zn: Sn: S = 2.2: 1.4: 1: 5.1. was comparable to the exact stoichiometric ratio – Cu: Zn: Sn: S = 2: 1: 1: 4. The copper, zinc, and sulphur rich CZTS thin films deposited from the chloride-based chemicals were in agreement with the findings of other researchers^{3, 18, 22, 24-27} and confirmed our deposited thin films' appropriateness

of high potency photovoltaic cells. However, Gua et al.⁵⁰ demonstrated that excess copper in the film can form binary and/or ternary stages of copper chalcogenide which deteriorated the device performance. Higher percentage of sulfur contents is probably responsible for higher bandgap energy (~1.5 eV) of the chloride chemical based CZTS thin films (1.65 eV).

IV Conclusions

In this paper, we have described a sol-gel dip-coating technique for productive CZTS thin film absorber layer solar cells. To know the carrier-induction and transportation process in the absorber layer, we studied the optical as well as the structural features of CZTS films. The optical study offered strong optical absorption ($0.4 \times 10^4 \text{ cm}^{-1}$) and nearly optimum bandgap energy (1.65 eV). The structural study confirmed the film's kesterite structure. The deposited films were compact and dense in nature. Large agglomerated particles distributed non-uniformly with well-defined boundaries, which give its advantage for solar cell application by reducing the recombination rate. Our research suggests a relatively straightforward, attainable and inexpensive technique for manufacturing CZTS films. As a whole, manufacturing process is innovative and versatile to malleable or rigid materials.

References

- Ginley, D., M. A. Green, and R. Collins, 2008. Solar Energy Conversion Toward 1 Terawatt. *MRS Bulletin*, **33(4)**, 355-364.
- Scragg J. J., P. J. Dale, L. M. Peter, G. Zoppi, and I. Probes, 2008. New routes to sustainable photovoltaics: evaluation of $\text{Cu}_2\text{ZnSnS}_4$ as an alternative absorber material. *physica status solidi (b)*, **245(9)**, 1772-1778.
- Jimbo, K., R. Kimura, T. Kamimura, S. Yamada, W.S. Maw, H. Araki, K. Oishi, and H. Katagiri, 2007. $\text{Cu}_2\text{ZnSnS}_4$ -type thin film solar cells using abundant materials. *Thin Solid Films*, **515(15)**, 5997-5999.
- Britt, J., and C. Ferekides, 1993. Thin-film CdS/CdTe solar cell with 15.8% efficiency. *Applied Physics Letters*, **62(22)**, 2851-2852.
- Khalate, S. A., R.S. Kate, and R.J. Deokate, 2018. A review on energy economics and the recent research and development in energy and the $\text{Cu}_2\text{ZnSnS}_4$ (CZTS) solar cells: A focus towards efficiency. *Solar Energy*, **169 (2018)** 616–633.
- Green, M. A., K. Emery, Y. Hishikawa, W. Warta, and E.D. Dunlop, 2016. *Solar cell efficiency tables (version 48)*.
- Guo, B. L., Y. H. Chen, X. J. Liu, W. C. Liu, and A. D. Li, 2014. Optical and electrical properties study of sol-gel derived $\text{Cu}_2\text{ZnSnS}_4$ thin films for solar cells. *AIP Advances*, **4(9)**, 097115.
- Katagiri, H., K. Saitoh, T. Washio, H. Shinohara, T. Kurumadani, and S. Miyajima, 2001. Development of thin film solar cell based on $\text{Cu}_2\text{ZnSnS}_4$ thin films. *Solar Energy Materials and Solar Cells*, **65(1)**, 141-148.
- Guo, Q., H. W. Hillhouse, and R. Agrawal, 2009. Synthesis of $\text{Cu}_2\text{ZnSnS}_4$ nanocrystal ink and its use for solar cells. *J Am Chem Soc*, **131(33)**, 11672-3.
- He, J., L. Sun, N. Ding, H. Kong, S. Zuo, S. Chen, Y. Chen, P. Yang, and J. Chu, 2012. Single-step preparation and characterization of $\text{Cu}_2\text{ZnSn}(\text{S}_x\text{Se}_{1-x})_4$ thin films deposited by pulsed laser deposition method. *Journal of Alloys and Compounds*, **529(Supplement C)**, 34-37.
- Shi, C., G. Shi, Z. Chen, P. Yang, and M. Yao, 2012. Deposition of $\text{Cu}_2\text{ZnSnS}_4$ thin films by vacuum thermal evaporation from single quaternary compound source. *Materials Letters*, **73(Supplement C)**, 89-91.
- Washio, T., T. Shinji, S. Tajima, T. Fukano, T. Motohiro, K. Jimbo, and H. Katagiri, 2012. 6% Efficiency $\text{Cu}_2\text{ZnSnS}_4$ -based thin film solar cells using oxide precursors by open atmosphere type CVD. *Journal of Materials Chemistry*, **22(9)**, 4021-4024.
- Banavoth, M., S. Dias, and S. B. Krupanidhi, 2013. Near-infrared photoactive $\text{Cu}_2\text{ZnSnS}_4$ thin films by co-sputtering. *AIP Advances*, **3(8)**, 082132.
- Tanaka, K., Y. Fukui, N. Moritake and H. Uchiki, 2011. Chemical composition dependence of morphological and optical properties of $\text{Cu}_2\text{ZnSnS}_4$ thin films deposited by sol-gel sulfurization and $\text{Cu}_2\text{ZnSnS}_4$ thin film solar cell efficiency. *Solar Energy Materials and Solar Cells*, **95(3)**, 838-842.
- Wang, Y., Y. Huang, A. Y. S. Lee, C. F. Wang, and H. Gong, 2012. Influence of sintering temperature on screen printed $\text{Cu}_2\text{ZnSnS}_4$ (CZTS) films. *Journal of Alloys and Compounds*, **539(Supplement C)**, 237-241.
- Yan, Z., A. Wei, Y. Zhao, J. Liu, and X. Chen, 2013. Growth of $\text{Cu}_2\text{ZnSnS}_4$ thin films on transparent conducting glass substrates by the solvothermal method. *Materials Letters*, **111(Supplement C)**, 120-122.
- Todorov, T. K., J. Tang, S. Bag, O. Gunawan, T. Gokmen, Y. Zhu, and D. B. Mitzi, 2013. Beyond 11% Efficiency: Characteristics of State-of-the-Art $\text{Cu}_2\text{ZnSn}(\text{S},\text{Se})_4$ Solar Cells. *Advanced Energy Materials*, **3(1)**, 34-38.
- Wang, W., M.T. Winkler, O. Gunawan, T. Gokmen, T. K. Todorov, Y. Zhu, and D. B. Mitzi, 2013. Device characteristics of CZTSSe thin-film solar cells with 12.6% efficiency. *Advanced Energy Materials* **4(7)**, 201301465.
- Jackson, P., D. Hariskos, R. Wuerz, and O. Kiowski, 2015. Cover Picture: Properties of $\text{Cu}(\text{In},\text{Ga})\text{Se}_2$ solar cells with new record efficiencies up to 21.7%. *Phys. Status Solidi RRL* **1/2015**.
- Kim, G. Y, D.-H. Son, T. T. T. Nguyen, S. Yoon, M. Kwon, C.-W. Jeon, D.-H. Kim, J.-K. Kang, and W. Jo, 2016. Enhancement of photo-conversion efficiency in $\text{Cu}_2\text{ZnSn}(\text{S},\text{Se})_4$ thin-film solar cells by control of ZnS precursor-layer thickness. *Progress in Photovoltaics: Research and Applications*. **24(3)**, 292-306.
- Mitzi, D. B., T. K. Todorov, K. Wang and S. Guha, 2011. The path towards a high-performance solution processed kesterite solar cell. *Solar Energy Materials and Solar Cell*, **95**, 1421–1436.
- Shin, B., O. Gunawan, Y. Zhu, N. A. Bojarczuk, S. J. Chey, and S. Guha, 2013. Thin film solar cell with 8.4% power conversion efficiency using an earth-abundant $\text{Cu}_2\text{ZnSnS}_4$ absorber. *Progress in Photovoltaics: Research and Applications*, **21(1)**, 72-76.
- Walsh, A., S. Chen, S.-H. Wei, and X.-G. Gong, 2012. Kesterite Thin-Film Solar Cells: Advances in Materials Modelling of $\text{Cu}_2\text{ZnSnS}_4$. *Advanced Energy Materials*, **2(4)**, 400-409.
- Polizzotti, A., I. L. Repins, R. Noufi, S.-H. Wei, and D. B. Mitzi, 2013. The state and future prospects of kesterite

- photovoltaics. *Energy & Environmental Science*, **6(11)**, 3171-3182.
25. Chen, S., A. Walsh, J.-H. Yang, X.G. Gong, L. Sun, P.-X., Yang, J.-H. Chua, and S.-H. Wei, 2011. Compositional dependence of structural and electronic properties of $\text{Cu}_2\text{ZnSn(S,Se)}$ (4) alloys for thin film solar cells. *Physical Review B*, **83(12)**, 125201
 26. Tanaka, T., D. Kawasaki, M. Nishio, Q. Guo, and H. Ogawa., 2006. Fabrication of $\text{Cu}_2\text{ZnSnS}_4$ thin films by co-evaporation. *physica status solidi (c)*, **3(8)**, 2844-2847.
 27. Katagiri, H., K. Jimbo, W. S. Maw, K. Oishi, M. Yamazaki, H. Araki, and A. Takeuchi, 2009. Development of CZTS-based thin film solar cells. *Thin Solid Films*, **517(7)**, 2455-2460.
 28. Hironori, K., J. Kazuo, Y. Satoru, T. Kamimura, W. S. Maw, T. Fukano, T. Ito, and T. Motohiro, 2008. Enhanced Conversion Efficiencies of $\text{Cu}_2\text{ZnSnS}_4$ -Based Thin Film Solar Cells by Using Preferential Etching Technique. *Applied Physics Express*, **1(4)**, 041201.
 29. Hsu, W. C, I. Repins, C. Beall, C. DeHart, B. To, W. Yang, Y. Yang, and R. Noufi, 2014. Growth mechanisms of co-evaporated kesterite: a comparison of Cu-rich and Zn-rich composition paths. *Progress in Photovoltaics: Research and Applications*, **22(1)**, 35-43.
 30. Fairbrother, A., E. Garcia-Hemme, V. Izquierdo-Roca, X. Fontane, F.A. Pulgarin-Agudelo, O. Vigil-Galan, A. Perez-Rodriguez and E. Saucedo, 2012. Development of a selective chemical etch to improve the conversion efficiency of Zn-rich $\text{Cu}_2\text{ZnSnS}_4$ solar cells. *J Am Chem Soc*, **134(19)**, 8018-21.
 31. Platzer-Björkman, C., J. Scragg, H. Flammersberger, D. Nam, M. Gansukh, H. Cheong, and J.-K. Kang, 2012. Influence of precursor sulfur content on film formation and compositional changes in $\text{Cu}_2\text{ZnSnS}_4$ films and solar cells. *Solar Energy Materials and Solar Cells*, **98(Supplement C)**, 110-117.
 32. Guan, Z., W. Luo, and Z. Zou, 2014. Formation mechanism of ZnS impurities and their effect on photoelectrochemical properties on a $\text{Cu}_2\text{ZnSnS}_4$ photocathode. *CrystEngComm*, **14**, 2929-2936.
 33. Jiang, M., Y. Li, R. Dhakal, and P. Thapalia, 2011. $\text{Cu}_2\text{ZnSnS}_4$ polycrystalline thin films with large densely packed grains prepared by sol-gel method. *J. of Photonics for Energy*, **1(1)**, 1-6.
 34. Kentaro, I., and N. Tatsuo, 1988. Electrical and Optical Properties of Stannite-Type Quaternary Semiconductor Thin Films. *Japanese Journal of Applied Physics*, **27(11R)**, 2094.
 35. Seol, J. S., S.-Y. Lee, J.-C. Lee, H.-D. Nam, and K.-H. Kim, 2003. Electrical and optical properties of $\text{Cu}_2\text{ZnSnS}_4$ thin films prepared by rf magnetron sputtering process. *Solar Energy Materials and Solar Cells*, **75(1)**, 155-162.
 36. Todorov, T. K., K. B. Reuter, and D. B. Mitzi, 2010. High-efficiency solar cell with Earth-abundant liquid-processed absorber. *Adv Materials*, **22(20)**, E156- E159.
 37. Tanaka, T., T. Nagatomo, D. Kawasaki, M. Nishio, Q. Guo, A. Wakahara, A. Yoshida, and H. Ogawa, 2005. Preparation of $\text{Cu}_2\text{ZnSnS}_4$ thin films by hybrid sputtering. *J. of Physics and Chemistry of Solids*, **66(11)**, 1978-1981.
 38. Tanaka, K., M. Oonuki, N. Moritake, and H. Uchiki, 2009. $\text{Cu}_2\text{ZnSnS}_4$ thin film solar cells prepared by non-vacuum processing. *Solar Energy Materials and Solar Cells*, **93(5)**, 583-587.
 39. Fischereder, A., T. Rath, W. Haas, H. Amenitsch, J. Albering, D. Meischler, S. Larissegger, M. Edler, R. Saf, F. Hofer, and G. Trimmel, 2010. Investigation of $\text{Cu}_2\text{ZnSnS}_4$ formation from metal salts and thioacetamide. *Chemistry of Materials*, **22(11)**, 3399- 3406.
 40. Pawar, S. M., B. S. Pawar, A. V. Moholkar, D. S. Choi, J. H. Yun, J. H. Moon, S. S. Kolekar, and J. H. Kim, 2010. Single step electrosynthesis of $\text{Cu}_2\text{ZnSnS}_4$ (CZTS) thin films for solar cell application. *Electrochimica Acta*, **55(12)**, 4057-4061.
 41. Pathan, H. M., and C. D. Lokhande, 2004. Deposition of metal chalcogenide thin films by successive ionic layer adsorption and reaction (SILAR) method. *Bulletin of Materials Science*, **27(2)**, 85-111.
 42. Thornton, J. A., 1986. The microstructure of sputter-deposited coatings. *Journal of Vacuum Science & Technology*, **4(6)**, 3059-3065.
 43. Tanaka, K., N. Moritake, and H. Uchiki, 2007. Preparation of $\text{Cu}_2\text{ZnSnS}_4$ thin films by sulfurizing sol-gel deposited precursors. *Solar Energy Materials and Solar Cells*, **91(13)**, 1199-1201.
 44. Pawar, B. S., S. M. Pawar, S. W. Shin, D. S. Choi, C. J. Park, S. S. Kolekar, and J. H. Kim, 2010. Effect of complexing agent on the properties of electrochemically deposited $\text{Cu}_2\text{ZnSnS}_4$ (CZTS) thin films. *Applied Surface Science*, **257(5)**, 1786-1791.
 45. Zhao, Y., H. Pan, Y. Lou, X. Qiu, J. J. Zhu, and C. Burda, 2009. Plasmonic $\text{Cu}_{(2-x)}\text{S}$ nanocrystals: optical and structural properties of copper-deficient copper(I) sulfides. *J Am Chem Soc*, **131(12)**, 4253-61.
 46. Ford, G. M, Q. Guo, R. Agrawal, H. W. Hillhouse, 2011. Earth Abundant Element $\text{Cu}_2\text{Zn(Sn}_{1-x}\text{Ge}_x)\text{S}_4$ Nanocrystals for Tunable Band Gap Solar Cells: 6.8% Efficient Device Fabrication. *Chemistry of Materials*, **23(10)**, 2626-2629.
 47. Caballero, R., C. Maffiotte, and C. Guillén, 2005. Preparation and characterization of $\text{CuIn}_{1-x}\text{Ga}_x\text{Se}_2$ thin films obtained by sequential evaporations and different selenization processes. *Thin Solid Films*, **474(1)**, 70-76.
 48. Riha, S.C., S. J. Fredrick, J. B. Sambur, Y. Liu, A. L. Prieto, and B. A. Parkinson, 2011. Photoelectrochemical characterization of nanocrystalline thin-film $\text{Cu}_2\text{ZnSnS}_4$ photocathodes. *ACS Appl Mater Interfaces*, **3(1)**, 58-66.
 49. Wangperawong, A., J. S. King, S. M. Herron, B. P. Tran, K. Pangan-Okimoto, and S. F. Bent, 2011. Aqueous bath process for deposition of $\text{Cu}_2\text{ZnSnS}_4$ photovoltaic absorbers. *Thin Solid Films*, **519(8)**, 2488-2492.
 50. Guo, Q., G. M. Ford, W.-C. Yang, B. C. Walker, E. A. Stach, H. W. Hillhouse, and R. Agawal, 2010. Fabrication of 7.2% Efficient CZTSSe Solar Cells Using CZTS Nanocrystals. *Journal of the American Chemical Society*, **132(49)**, 17384-17386.
 51. Nazligul, S. A., M. Wang and L. K. Choy, 2020. Recent Development in Earth-Abundant Kesterite Materials and Their Applications. *Sustainability*, **5138(12)**, 1-19.
 52. Abdelraouf, O. A. M., and N. K. Allam, 2017. Plasmonic scattering nanostructures for efficient light trapping in flat CZTS solar cells. *Proc. of SPIE*, **10227(12)** 1-9
 53. Khalate, S. A., R. S. Kate, R. J. Deokate, 2018. A review on energy economics and the recent research and development in energy and the $\text{Cu}_2\text{ZnSnS}_4$ (CZTS) solar cells: A focus towards efficiency. *Solar Energy*, **169(2018)** 616-633